Fabrication of well-ordered titania nanotubes by three-step anodization in lactic acid-containing electrolytes

PENG WANG*, PENGFU LIU, WEI LIU, SHUHUA TENG
School of Materials Science and Engineering, China University of Mining and Technology, Xuzhou 221116, China

Well-ordered titania nanotube arrays (TNAs) were successfully synthesized by three-step anodization in the ethylene glycol-based electrolytes containing lactic acid. The tube length of TNAs was found to be almost linearly dependent on the anodization temperature when the potential difference was kept constant at 60 V. However, their pore diameter reached a maximum at 40°C and then decreased with increasing temperature. The addition of lactic acid to the electrolytes greatly improved the morphology of TNAs, producing well-ordered nanotubes with ripples on the walls. Moreover, the XRD results showed that the crystal structure of TNAs was closely related to the annealing temperature. The growth mechanism of TNAs in the presence of lactic acid was also explained.

(Received May 13, 2016; accepted November 25, 2016)

Keywords: Titania nanotubes, Three-step anodization, Temperature, Lactic acid

1. Introduction

Over the past decade, titania nanotube arrays (TNAs) have attracted increasing attention in the fields of dye-sensitized solar cells (DSSCs) [1], degradation of organic pollutants [2-5], gas sensing [6], and water splitting [7] due to their unique structure, large surface area and good performances. For all these applications, the performances of TNAs are strongly dependent on their structures. Therefore, numerous efforts have been made on structural investigations of TNAs not only by control over their morphology (diameter, length, smoothness, and so on), but also by a mechanistic understanding of crucial factors for growth [8-10]. To obtain highly ordered TNAs, a multi-step anodization strategy has been developed, which is similar to a self-organized anodization of aluminum [11]. However, this approach is not very often presented in the literatures due to the problem with an effective removal of the oxide layer without disturbance to the titanium base. Especially, the correlations between the structural dimensions of TNAs and the anodization temperature have been rarely explored when multi-step anodization is applied.

In the present work, the ethylene glycol (EG)-based electrolyte containing lactic acid (LA) was used to prepare well-ordered TNAs through a three-step anodization process. The influence of the anodization temperature on the pore diameter and tube length of TNAs was investigated. The crystal structure of TNAs annealed at different temperatures was analyzed by XRD. Moreover, the growth mechanism of TNAs in the EG/LA systems was also explained.

2. Experimental procedure

Titania nanotubes were fabricated by three-step anodization according to the following procedures: Firstly, pure titanium foils (Baoji Haode Titanium Industry Co., Ltd) were pretreated by mechanical and chemical polishing, followed by ultrasonic cleaning. Subsequently, anodization of the titanium foils was performed in a home-made Teflon electrochemical cell (100 cm^3). The electrolyte consisted of ethylene glycol, 0.3 wt% ammonium fluoride (NH_4F), 2 vol% distilled water and 1.5 mol/L lactic acid. A titanium plate and platinum grid served as the anode and cathode, respectively, with a distance of 2 cm between the two electrodes. The potential difference was constant at 60 V, and the anodization temperature was varied from 20°C to 50°C. Each anodizing step was followed by a mechanical removal of the grown oxide layer via ultrasonic agitation. After the third anodizing step, the samples were rinsed with distilled water, dried in the air and then calcined for 2 h in a muffle furnace. The morphology of TNAs was viewed by field emission scanning electron microscopy (FESEM, JSM-6700F). The crystal structure was measured by X-ray diffraction (XRD, D8 Advance). Image J 1.37v software was used to estimate the pore diameter and tube length of TNAs.

3. Results and discussion

Fig. 1 shows the typical top-view SEM images of TNAs prepared at different stages of anodization when lactic acid was contained in the EG-based electrolyte. The voltage was set at 60 V and the anodization temperature was 40°C. It was observed in Fig. 1(a) that one-step anodization resulted in TNAs with small diameters, and the tubes were intensively piled up together. By contrast, the obtained TNAs via two-step anodization displayed a much clearer tubular structure and larger inner diameter (Fig. 1(b)). This may be because that the generated periodic concave on the metal surface by removal of the first oxide layer could serve as the nucleation sites of TNAs during the second anodization step. After three-step anodization, the cross-section of those TiO_2 nanotubes exhibited an approximately hexagonal honeycomb-like pattern, as presented by their top-view SEM image in Fig. 1(c). Moreover, their inner diameter increased significantly as compared to those shown in Figs. 1(a) and 1(b).

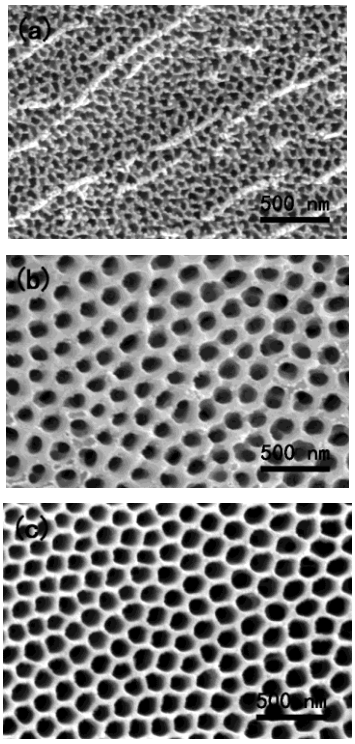

Fig. 1. Top-view SEM images of TNAs formed on the Ti substrate via (a) one-, (b) two-, and (c) three-step anodization in the EG -based electrolyte containing lactic acid at 60 V and 40°C

The EG-based electrolytes with and without the addition of lactic acid were applied to prepare TNAs by three-step anodization. Fig. 2 shows the cross-sectional and top-view SEM images of TNAs formed in two different electrolytes at 60 V and 40°C. The vertically aligned TNAs were always obtained regardless of the presence of lactic acid. However, it can be clearly seen in Figs. 2(a) and 2(b) that, when lactic acid was absent from the electrolyte, the tubular morphology was poor, and the cross-section of the nanotubes demonstrated a porous, sponge-like structure. In contrast, the anodization in the EG-based electrolyte containing lactic acid led to the formation of a closely packed, honeycomb-like surface morphology (Fig. 2(c)). Moreover, the tubular structure of the as-prepared TNAs became uniform and highly ordered, with the pore diameter ranging from 200 to 250 nm. Besides, the tube surface exhibited ripples on the walls, and the outer diameter of TNAs was constant over their entire length. It was thought that the addition of lactic acid changed the viscosity of the EG-based electrolyte, thus eventually achieving TNAs with different morphologies.

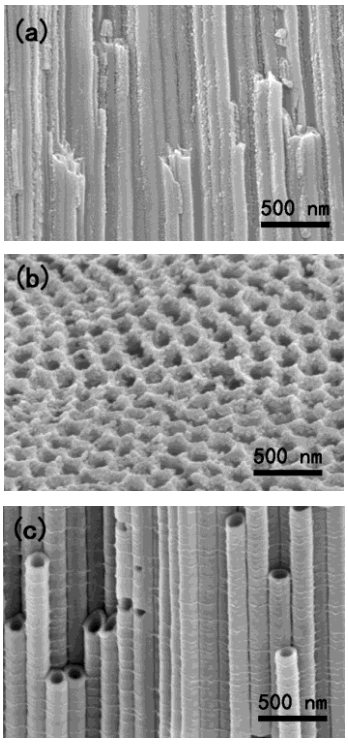

Fig. 2. Cross-sectional and top-view SEM images of TNAs formed by three-step anodization in the EG-based electrolyte (a, b) without and (c) with the addition of lactic acid

The XRD diagrams of TNAs annealed at different temperature are displayed in Fig. 3. No diffraction peaks were detected in the XRD pattern of TNAs before calcination, suggesting their amorphous structure. By contrast, the TNAs annealed at 200°C showed a typical anatase phase, characterized by the existence of the main diffraction peaks at 25.4° and 48.1° for the (101) and (200) crystal planes of anatase TiO_2, respectively. The intensity of those diffraction peaks were significantly enhanced at 400°C, and a small diffraction peak of the rutile phase at

27.2° was also observed. A further increase of annealing temperature to 600°C led to the appearance of more diffraction peaks of the rutile phase. At 800°C, the diffraction peaks of the anatase phase either diminished in intensity or disappeared, while the diffraction intensity of the rutile phase was further strengthened due to the phase transformation. The above results indicated that the crystal structure of TNAs was greatly dependent on the annealing temperature. As the annealing temperature was increased, the anatase phase was gradually transformed to the rutile phase. Therefore, it was desirable to obtain anatase or mixed anatase/rutile TNAs by varying the annealing temperature for different applications.

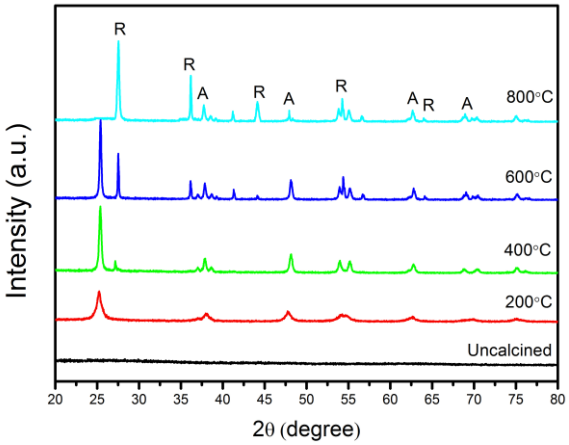

Fig. 3. XRD patterns of TNAs under different annealing temperature (A-anatase, R-rutile)

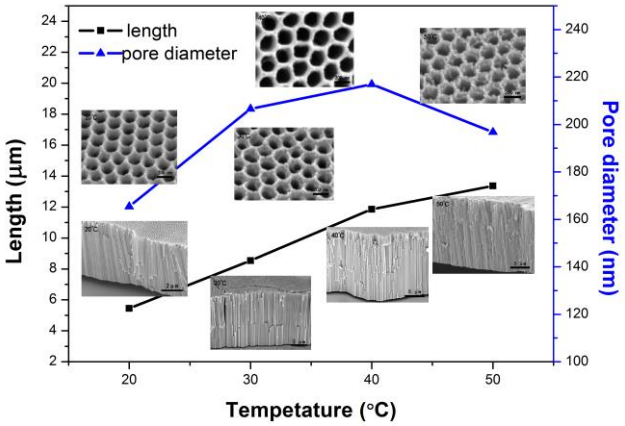

Fig. 4. Variations of the length and pore diameter of TNAs with the anodization temperature. The insets show the typical SEM images of the obtained TNAs

Fig. 4 exhibits the impacts of the anodization temperature on the morphological parameters of TNAs at a voltage of 60 V. Two parameters including tube length and pore diameter of TNAs were estimated from the SEM images using an appropriate software. It was revealed from Fig. 4 that both the tube length and pore diameter significantly increased when the temperature rose from 20°C to 40°C. It has been reported that the viscosity of the non-aqueous electrolyte was inversely proportional to the rate of the tube growth in the diffusion controlled anodization process [12,13]. In the present system, the viscosity of the electrolytes decreased with the increase of temperature. Therefore, the diffusion-dominated local acidification at the tube bottom was promoted, and the rate of the tube formation accordingly increased. Upon further increase of the anodizing temperature from 40°C to 50°C, the tube length continued to increase while the pore diameter decreased surprisingly. It was possibly ascribed to the enhanced hydrolysis of the Ti^{4+} ions in the electrolyte as a consequence of the increase in the growth rate of TNAs at higher temperature [14]. Correspondingly, the hydrolysis led to the precipitation of hydrous titanium dioxide on the TNAs surface, therefore reducing their pore diameter. Ultimately, it was concluded that the optimal temperature for growth of TNAs was 40°C at a given potential difference of 60 V.

The anodic growth of TNAs was thought to involve three stages. Moreover, the morphological evolution of TNAs occurring in these stages is actually a result of the competition between electrochemical etching process and chemical dissolution process on titanium [15,16]. Based on the above observations under different conditions, a possible growth mode was proposed to explain the formation of TNAs in the EG-based electrolyte containing lactic acid. The oxide growth initially occurred on the substrate surface due to the interaction between the Ti metal and the produced O^{2-} or OH^- ions by water decomposition. Afterwards, under an electric field, the resultant metal ions (Ti^{4+}) by dissolution of the oxide will move from the metal-oxide interface to the oxide-electrolyte (OE) interface. Except for the field-assisted dissolution of the oxide at OE interface, chemical dissolution of the oxide by lactic acid also took place during anodization, leading to the formation of pore channels. In the EG-based electrolyte containing lactic acid, H^+ ions came from not only water decomposition at the tube bottom but also the ionization of lactic acid in the electrolyte. With the aid of lactic acid, chemical dissolution of TiO_2 can be easily to keep a balance with the electrochemical etching process, which will accordingly ensure the stable growth of TNAs. As the anodization proceeded, the ‘plastic flow’ of the newly formed oxide will eventually give rise to a tubular thin layer on the substrate [17]. Moreover, the presence of lactic acid may play an important role in optimizing the ‘plastic flow’ process by adjusting the viscosity of the EG-based electrolytes, thus achieving regularly tubular morphology of TNAs as compared to those obtained without adding lactic acid.

4. Conclusions

Well-ordered TiO_2 nanotube arrays were generated in the EG-based electrolyte containing lactic acid by

three-step anodization. As compared to those prepared without the addition of lactic acid, the TiO_2 nanotubes displayed a greatly improved tubular morphology. Moreover, with the increase of the anodizing temperature from 20°C to 50°C, the tube length showed an almost linear increase, while the pore diameter was found to decrease at high temperature. The best tube arrangement was formed in a controlled manner by anodization at 60 V and 40°C in the lactic acid-contained electrolyte. In addition, anatase TiO_2 was gradually transformed to a rutile phase as the annealing temperature was increased. The as-prepared TiO_2 nanotubes are expected to find potential applications in the fields of photocatalysis, DSSCs and biomedicine.

Acknowledgements

This work was financially supported by the Fundamental Research Funds for the Central Universities (No. 2013QNA06).

References

[1] F. Bella, A. Lamberti, A. Sacco, S. Bianco, A. Chiodoni, R. Bongiovanni, J. Membrane Sci. **470**, 125 (2014).
[2] F. Zhang, C.-L. Zhang, W.-N. Wang, H.-P. Cong, H.-S. Qian, Chem. Sus. Chem. **9**, 1449 (2016).
[3] I. Paramasivam, H. Jha, N. Liu, P. Schmuki, Small **8**, 3073 (2012).
[4] D. Yang, Y. Y. Sun, Z. W. Tong, Y. Tian, Y. B. Li, Z. Y. Jiang, J. Phys. Chem. C **119**, 5827 (2015).
[5] F. Zhang, C.-L. Zhang, H.-Y. Peng, H.-P. Cong, H.-S. Qian, Part Part Syst. Charact. **33**, 248 (2016).
[6] V. Galstyan, E. Comini, G. Faglia, G. Sberveglieri, Sensors **13**, 14813 (2013).
[7] S. K. Mohapatra, M. Misra, V. K. Mahajan, K. S. Raja, J. Cataly. **246**, 362 (2007).
[8] P. Roy, S. Berger, P. Schmuki, Angew Chem.-Int. Edit. **50**, 2904 (2011).
[9] P. Van Viet, B. T. Phan, L. V. Hieu, C. M. Thi, J. Nanosci. Nanotechnol. **15**, 5202 (2015).
[10] J. Lin, X. Liu, S. Zhu, Y. Liu, X. Chen, J. Nanomater. 9 (2015).
[11] G. D. Sulka, W. J. Stepniowski, Electrochim. Acta **54**, 3683 (2009).
[12] J. M. Macak, H. Hildebrand, U. Marten-Jahns, P. Schmuki, J. Electroanal Chem. **621**, 254 (2008).
[13] J. M. Macak, P. Schmuki, Electrochim. Acta **52**, 1258 (2006).
[14] D. Wang, Y. Liu, B. Yu, F. Zhou, W. Liu, Chem. Mater. **21**, 1198 (2009).
[15] J. Tao, J. Zhao, C. Tang, Y. Kang, Y. Li, New J. Chem. **32**, 2164 (2008).
[16] D. Guan, Y. Wang, Nanoscale **4**, 2968 (2012).
[17] S. Berger, S. P. Albu, F. Schmidt-Stein, H. Hildebrand, P. Schmuki, J. S. Hammond, D. F. Paul, S. Reichlmaier, Surf. Sci. **605**, L57 (2011).

*Corresponding author: wp425@cumt.edu.cn